Smart Structures and Systems, *Vol. 26, No. 3 (2020) 391-401*
DOI: https://doi.org/10.12989/sss.2020.26.3.391

Analytical evaluation and experimental validation of energy harvesting using low-frequency band of piezoelectric bimorph actuator

Kaushik Mishra [1a], Subrata K. Panda*[2], Vikash Kumar [2b] and Hukum Chand Dewangan [2c]

[1] *School of Mechanical Engineering, VIT Vellore, Vellore-632014, Tamil Nadu, India*
[2] *Department of Mechanical Engineering, NIT Rourkela, Rourkela-769008, Odisha, Sundergarh, India*

(*Received March 10, 2020, Revised May 16, 2020, Accepted May 29, 2020*)

Abstract. The present article reports the feasibility of the electrical energy generation from ambient low-frequency vibration using a piezoelectric material mounted on a bimorph cantilever beam actuator. A corresponding higher-order analytical model is developed using MATLAB in conjunction with finite element method under low-frequency with both damped and undamped conditions. An alternate model is also developed to check the material and dimensional viability of both piezoelectric materials (mainly focussed to PVDF and PZT) and the base material. Also, Genetic Algorithm is implemented to find the optimum dimensions which can produce the higher values of voltage at low-frequency frequencies (≤ 100 Hz). The delamination constraints are employed to avoid inter-laminar stresses and to increase the fracture toughness. The delamination has been done using a Teflon sheet sandwiched in between base plates and the piezo material is stuck to the base plate using adhesives. The analytical model is tested for both homogenous and isotropic material characteristics of the base material and extended to investigate the effect of the different geometrical parameters (base plate dimensions, piezo layer dimensions and placement, delamination thickness and placement, excitation frequency) on the model responses of the bimorph cantilever beam. It has been observed that when the base material characteristics are homogenous, the efficiency of the model remains higher when compared to the condition when it is of isotropic material. The necessary convergence behaviour of the current numerical model has been established and checked for the accuracy by comparing with available published results. Finally, using the results obtained from the model, a prototype is fabricated for the experimental validation via a suitable circuit considering Glass fibre and Aluminium as the bimorph material.

Keywords: piezoelectric materials; PZT; PVDF; bimorph actuator; glass fibre

1. Introduction

Energy has always been the most demanding factor in our daily life. All our house-hold works are centred towards operations that deal directly with electrical energy. In the past, varieties of techniques have already been adopted to gain electrical energy which includes electromagnetic induction (Glynne-Jones *et al*. 2004), electrostatic generation (Mitcheson *et al*. 2004) and the intervention of piezoelectric material (Arul *et al*. 2019, Dash and Singh 2009). The piezoelectric material applications to improve the frequency responses have also been received larger attention due to their multifaceted applications i.e., actuators, sensors, conductors etc. (Najini and Muthukumaraswamy 2017). This, in turn, allows to develop a conceptual simulation model for the generation of energy from the vibrations of road traffic via the piezoelectric materials. Moreover, the research relevant to the micro-electro-mechanical model (Arani *et al*. 2016) of the composite plate embedded with piezoelectric material under the combined mechanical and electrical loading. Also, the harvesting of energy can be achieved by embedding piezoelectric transducer in the soldier's boot soles to capture the energy generated due to the gait motion (Othman 2017). In addition, the energy could be harvested from the different activities of human organism i.e., heart and lungs by using the piezoelectric based harvesters (Dagdeviren *et al*. 2014). The study proposes the possibility of the harvested energy could be supplied to powering the micro batteries associated with the artificial organs within the human body. Further, novel modelling approach has been adopted (Singh and Panda 2017) for the prediction of frequency responses and subsequent improvement considering the PZT layer embedding due to the induction of large deformation. Similarly, the nonlinear natural frequency of the composite embedded with piezoelectric material reported (Mohammadzadeh-Keleshteri *et al*. 2017) considering the lower-order theory (first-order shear deformation theory, FSDT) and von-Karman type of non-linearity strain-displacement relations. A novel integral technique in conjunction with the FSDT is proposed to predict the eigenvalues (buckling and vibration) of the composite (Bousahla *et al*. 2020, Rahmani *et al*. 2020, Sahla *et al*. 2019 and Tlidji *et al*. 2019) and graded carbon nanotube reinforced beam (Motezekar and Eyvazian 2020) structure. Further, some more research articles (Kaddari *et al*. 2020, Mahmoudi *et al*. 2017, Zaoui *et al*. 2019 and Boukhlif *et al*.

*Corresponding author, Ph.D., E-mail: call2subrat@gmail.com; pandask@nitrkl.ac.in
[a] Research Scholar, E-mail: kaushikmishra77@gmail.com
[b] Resaerch Scholar, E-mail: vikashkr050sagar@gmail.com
[c] Research Scholar, E-mail: hukumdewangan@gmail.com

http://www.techno-press.org/?journal=sss&subpage=7 ISSN: 1738-1584 (Print), 1738-1991 (Online)

2019) proposed a new type of quasi shear deformation theory to evaluate the structural responses i.e., the static and free vibration frequencies of the functionally graded porous plate resting on the elastic foundations. Similarly, the strain gradient theory has been adopted to compute the eigenvalue type of buckling of the functionally graded micro beam or micro bar structure (Akgöz and Civalek 2013, Civalek and Akgöz 2014) using a non-trivial solution technique for variable structural configurations (cantilever and propped cantilever beam). Moreover, the effect surface stresses on the eigenvalues and static deflection i.e., increase (frequency and buckling load) or decrease behaviour reported by Motezaker *et al*. (2020). Also, a few research relevant to frequency responses of functionally graded material (FGM) structure are reported using the variable kinematic model includes the refined integral theory (Balubaid *et al*. 2019 and Berghouti *et al*. 2019). It was noted that the frequencies predicted using the classical models are predominant for lower order frequency values in comparison to the adopted one. The potential induced due to the bending deformation in multilayer smart composite piezo-laminated cantilevered cylindrical shell panel investigated further by Balamurugan and Narayanan (2009) considering the electric field for different values of piezo thickness and shell curvature. Rafiee *et al*. (2013) presented an analytical technique to obtain the linear and nonlinear free and forced vibration responses of piezoelectric bonded functionally graded material (FGM) shell structure subjected to the combined loading, i.e., electrical, mechanical, thermal and aerodynamic. Micro and nano-based actuators find a wide range of applications related to the Micro Electro Mechanical Systems (MEMS) are mainly utilized in temperature sensors (Moser and Gijs 2007). Other applications of nanobeam actuators include applications in electrostatic actuators (Hung and Senturia 1999) and in ultra-microscopy (Li *et al*. 2003) which is broadly categorized as the Nano Electro-Mechanical Systems (NEMS). Based on the available research, it can be concluded that the research relevant to energy harvesting under the low-frequency range have been attracting the attention of different researchers. However, the study relevant to the energy harvesting considering the unconventional material and their modelling are limited in number. Hence, the main challenge is to construct a model that can simulate the vibration upon a given frequency bandwidth and conversion of energies, i.e., mechanical to electrical. Cantilever structure is a widely used geometry in piezoelectric energy harvesters.

The models for the cantilever type piezoelectric harvesters are defined using the variable mathematical expressions (Roundy and Wright 2004, Aridogan *et al*. 2014, Erturk and Inman 2009, Shutao *et al*. 2012, Shu and Lien 2006) to compute the desired output. Additionally, a few research indicates (Li *et al*. 2014) that a large mechanical strain can be produced within the piezoelectric layer due to the vibration. Another important aspect for choosing a cantilever beam geometry is relatively simple design. Similarly, the usage of tuning tip mass (Dechant *et al*. 2017) may useful for the optimal frequency generation in the bimorph system. The resonance frequency of the fundamental modes (Li *et al*. 2014) of a cantilever is lower than that of the modes obtained from the piezoelectric element. The models are categorised into two types based on either distributed parameter modelling (Shutao *et al*. 2012, Erturk and Inman 2008) or lumped parameter modelling (Dutoit *et al*. 2005 and Kim et *al*. 2015). The lumped parameter modelling is derived and implemented by Roundy and Wright (2004) as well as Dutoit *et al*. (2005). The lumped parameter modelling offers the simple kind of usage, which, in turn, has its own advantage. But the usage is limited to the fundamental mode of vibration only (Kong *et al*. 2014). The effect of electromechanical coupling factor in the piezoelectric material plays an important role in the modelling of the energy harvester (Zhu *et al.* 2009).

Further, a bimorph piezoelectric cantilever with end mass has been investigated (Kundu and Nemade 2016) as the energy harvester. Piezoelectric bonded cantilever with Silicon proof mass is designed and fabricated for the low-frequency vibration energy harvesting. In this regard, a few types of research have been done with relevance to the piezoelectric laminated cantilever, design and fabrication to harvest energy (Khalatkar *et al*. 2014 and Muralt *et al*. 2009). The energy harvesting by PZT (Lead Zirconium Titanate) unimorphs is presented considering the frequency data by a different researcher (Panda *et al*. 2018 and Shen *et al*. 2009). Besides, large numbers of attempts have also been made in the past (Bellal *et al*. 2020, Asghar *et al*. 2020, Taj *et al*. 2020, Balubaid *et al*. 2019, Hussain *et al*. 2019) to model the structural components made up of various advanced type structural material (Boutaleb *et al*. 2019, Berghouti *et al*. 2019, Semmah *et al*. 2019, Bedia *et al*. 2019) considering different kinds of kinematic models considering the shear-deformation effects (Karami *et al*. 2019a, b, c, d, e) and lower-order theories with adequate accuracy.

In this regard, a bimorph actuator model has been developed analytically, owing to its high response rate and easier implementation. PZT has been chosen as the right type of piezo material over PVDF (polyvinylidene fluoride) due to its high dielectric ratio. Due to their high strain response factor, it can be conveniently used for the harvesting of electrical energy from the vibrational frequencies. In this regard, a cantilever beam is chosen with a point load and solved analytically to compute its frequency response. Now, a PZT patch has been stuck on the beam surface using the adhesives (Araldite) for subsequent analysis, i.e., the analytical (using MATLAB environment and commercial ANSYS software). The base material of the cantilever can be simulated for various isotropic and homogenous materials (Aluminium, structural steel and glass fibre), out of which glass fibre is chosen due to the optimum desired result. Further, the model validity has been verified by comparing the responses with published data. Finally, to show the model accuracy a circuit has been fabricated with optimal geometrical dimensions (using Genetic Algorithm) and utilised for the experimental verification purpose. In the final section, a sample prototyping is done, which can be employed in practical usage.

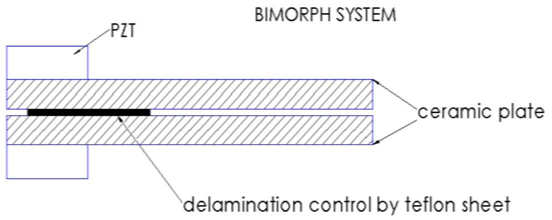

Fig. 1 A simple bimorph system

2. Design consideration of Bimorph Actuator

There are three types of modelling steps adopted for the Bimorph beam design. In this analysis, the analytical model of transducer type de-laminated ceramic beam or Bimorph Actuator has been developed and can be seen in Fig. 1.

Bimorph Actuator: This employs a rectangular plate which has PZT material adhered on both sides of the plate. In order to introduce delamination, we use a thin layer of Teflon coating in between the base plate. A small mass is placed at the free end of the plate which will act as a partial accelerometer and help in keeping the frequency of vibration in the desired range.

In the past, many researchers have adopted different solution techniques including the theories to compute the strain energies in the beam as well as compute the voltage generated from the corresponding vibration and few important contributions are discussed here to present the necessity of the current analysis. Finite Element Analysis (FEA) of an axially Functionally Graded (FG) piezo laminated cantilever beam with various shape variations using the Euler–Bernoulli beam theory and Genetic Algorithm-based constrained optimisation scheme for the harvesting of optimal vibrational energy of such piezo laminated beam arecompleted (Biswal *et al*. 2017). Also, the finite element (FE) simulation model is developed by (Singh *et al*. 2016) with the help of a commercial numerical tool (MATLAB) to investigate the geometrically nonlinear transient behaviour of the laminated composite plate embedded with the smart layer for the sensor and the actuator configuration. A brief comparison on various model of a piezo material are compared (Caliò *et al*. 2014) which are notably d_{33}, d_{31} and d_{15}. Although d_{15} is found to be the most efficient mode for research but d_{33} is found to give out highest outputs of voltage which again shifts the focus as our primary aim remains to achieve higher voltages. In Yang (2010), a brief calculation for voltage outputs and corresponding efficiency calculations have been done for a fabricated layer 3-D MEMS plate. Further extrapolation of the results yielded that homogenous materials could have a higher efficiency than conventionally used isotropic materials. This work majorly deals in comparison of the axiom that homogenous materials like carbon and glass fibres could when used as material for base plate in a bimorph actuator is more efficient than using isotropic material like steel or aluminium. Further an analytical model has been developed to form a foundation to the above axiom. Experimental works are carried out to support the analytical model. The only problem that could arise is the variation in directional properties but thius was ruled out by Josefsson (2014) stating that base plate can only have 2DOFs. Timoshenko and Euler-Bernoulli beam theory are employed as has been done by Biswal *et al*. (2017) because they are less complicated and only deal with variables that directly govern the actuating phenomenon. Another major problem that arises when using homogenous material is its elastic fracture. This problem has been thoroughly answered by Zeng *et al*. (2018) wherein they employed the principle of delamination by using a thin Teflon sheet in between the sandwiched layers. Similar theory has been adopted by using a delamination layer of Teflon sheet in between the sandwiched base plate.

3. Analytical modelling

The mechanical and electrical aspects of the system are obtained considering the material properties, geometries and the loading conditions via the analytical modelling space. In this regard, the space variation model of the beam is expressed using Euler Bernoulli beam equation.

$$\frac{\delta^2}{\delta x^2}\left[EI\frac{\delta^2 w}{\delta x^2}\right] = q \tag{1}$$

Now, resolving the load in terms of moment ('*M*') yields a more convenient form of Euler-Bernoulli beam equation and conceded to the following form

$$M = -EI\,\frac{\delta^2 w}{\delta x^2} \tag{2}$$

where, 'q' and 'w' are the load and deflection values of the system respectively.

The fundamental law of energy conservation in association with Hamilton principle is employed to express the system governing the equation of motion

$$d\varphi = \int_{t_1}^{t_2} \partial\left(T_k - T_p + W_e\right)dt = 0 \tag{3}$$

Where, 'T_k', 'T_p' and 'W_e' are the total kinetic energy, total potential energy and the external work done.

3.1 Piezo material selection and modelling:

The properties for the Piezo material is obtained considering the following mathematical expressions

$$Y(x) = Y_0\left[1 - \frac{x}{(K+1)^2}\right]^{np} \tag{4}$$

where, 'Y_0' is the property of parent material at x = 0; similarly, the gradient 'np' is the index and integer parameter 'K' utilizes to obtain the final expression.

Similarly, the average strain rate coefficient can be expressed as a function of Piezo material properties as given in Eq. (5).

$$s(x) = \frac{M}{EI} \times (Y(x) - Y_0) \tag{5}$$

Table 1 Strain rate coefficient values of various piezo materials

Material	d_{33} (C/N)
Quartz	23×10^{-13}
$BaTiO_3$	90×10^{-12}
$PbTiO_3$	12×10^{-12}
PVDF	475×10^{-12}
PZT	5.6×10^{-10}
PZT-5H	2500×10^{-12}

Now, the necessary straining rate has been computed for different harvesting materials via above two equations. Hence, Eq. (4) is employed in Eq. (5) and the outcome of each material, i.e., PZT, PVDF and PZT-5H. The output of the expression indicates PZT-5H has a better strain rate coefficient while compared to other two.

The variation of strain profiling with the associated parameter is determined by the following conditions: for linear profiling n = 1, for parabolic profiling n = 2 and for cubic profiling n = 3. For simplicity of experimentation, the linear profiling is chosen. To achieve the necessary condition the dielectric induced field constants are d_{31}, d_{33} and d_{15}. The subscript associated with the constant terms indicate the electric field induction direction and the corresponding strain.

3.2 Beam modelling

Beam Modelling can be done by using the governing analytical relation as per tapering constants

$$A(x) = A_0\left(1-\frac{C_b x}{L}\right)^n\left(1-\frac{C_h x}{L}\right)^n \tag{6}$$

Where, C_b is taper ratio for breadth and C_h is taper ratio for height.

Stress on PZT is obtained by employing the strain-rate values and the corresponding deflection, the relation between the three parameters can be established as

$$r(x) = \frac{\delta^2 w}{\delta x^2} \tag{7}$$

Further, simplifying the deflection value in terms of base acceleration ('q_i') and nodal frequency ('N_v'), the stress equation can be modified to the following form

$$r(x) = \frac{\delta^2[N_v * q_i]}{\delta x^2} \tag{8}$$

But the above obtained stress function gives the instantaneous rate of stress at any point along the x-direction from the origin. Hence, the average stress function is obtained by integrating the instantaneous stress rate along the full length L_p and conceded as

$$\overline{r}(x) = 1/L_p\int_0^{L_p}\frac{\delta^2[N_v * q_i]}{\delta x^2}dx \tag{9}$$

To obtain the optimal geometrical parameters, Genetic algorithm is adopted for the evaluation of the taper ratio breadth (C_b), taper ratio height (C_h), load resistance (R_L), piezo layer thickness (t_p) and the power gradient indices (n_p), Integer parameter (K) is simplified further to compute the efficiency value. The efficiency gives out the ratio between the net voltages gains to the piezo setup and the accelerated vibration induced via the bimorph actuator system.

Efficiency calculation

$$\eta = \left(\int_{t_1}^{t_2}\frac{V_{RL}(t)^2 dt}{R_L}\right)\times\frac{100}{\frac{s(D_1^2-D_2^2)}{2}} \tag{10}$$

where, D_1 and D_2 are peak deflections at time t_1 and t_2. Also, the deflection is computed to measure the acceleration due to the induced vibration at any instant of time. The constant 'S' is referred to as the effective spring constant of the cantilever plate. The plate is considered to be a simple damped spring with varying damping factor. $V_{RL}(t)$ represents the voltage gain across R_L. Solving the Eq. (9) yields that maximum value of Efficiency, η occurs at resonating frequency (f_R) at a particular value of load resistance, $R_L = \frac{1}{2\pi\varepsilon_0 f_R}$

The theoretical efficiency equation in terms of k^2 (electromechanical coupling coefficient) yields

$$\eta = \frac{\left(\frac{1}{2}\right)\left[\frac{k^2}{1-k^2}\right]}{\left(\frac{1}{Q}\right)+\left(\frac{1}{2}\right)\left[\frac{k^2}{1-k^2}\right]}\times 100 \tag{11}$$

where, 'Q' is quality factor which considers the net loss of energy during the vibration and out of the input range for the piezo layer.

For low-frequency ceramic plates, the electromechanical coupling coefficient can be written as a function of directional induced field coefficients (d_{31} and C_{11}^E) and static induced field coefficient (S_{33}^T)

$$k_{31}^2 = \frac{d_{31}^2}{C_{11}^E S_{33}^T} \tag{12}$$

The whole system can be assumed to be of a one-dimensional spring mass system with a relative ground

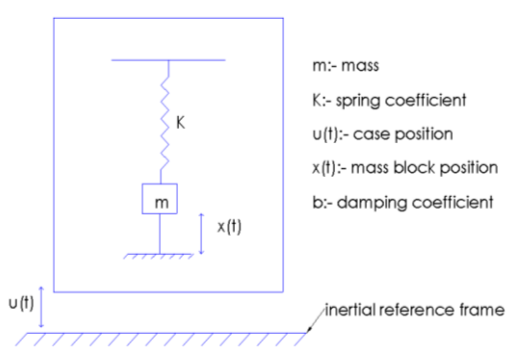

Fig. 2 Representation of vibration system in the form of spring mass system

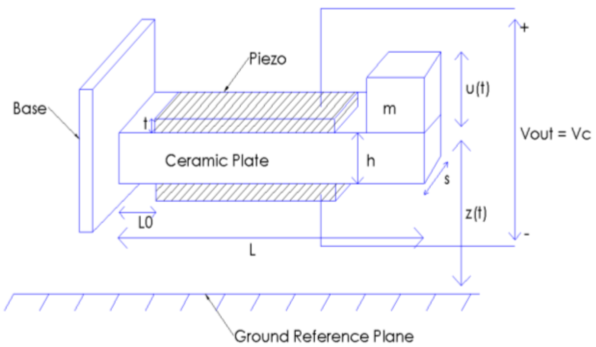

Fig. 3 The modelled bimorph actuator

reference as shown in Fig. 2. This is to make the modelling and scaling easier to deal with thus paving away all the difficulties that arise during the subsequent modelling of the actual bimorph system.

The main aim is to excite the damper at a frequency that is close to its natural frequency, in this way we get maximum power output.

$$Y = A\omega^2 \tag{13}$$

If $\omega = \omega_n$, it results in resonance; thus, it can be written as $\omega_n = \sqrt{\frac{k}{m}}$. Then peak power, P_d assumes the form as

$$P_d = \frac{mA^2}{4\omega_n \varepsilon_t} \tag{14}$$

Consider all the point masses ('m') accumulated at a single point which acts along a perpendicular axis along the cantilever as shown in Fig. 3

$$M = \beta_m(m_\phi + m_b) + m_a \tag{15}$$

Eq. (15) depicts the mass distribution along the length of the cantilever.

The spring constant of the whole damper system if compared to one-dimensional spring mass system, yields

$$K = \beta_k\left(\frac{2t^3}{3L^3} + \frac{ht^2}{L^3} + \frac{th^2}{2L^3}\right)C_{p11}^E + \frac{h^3}{12L^2}C_{b11}^E \tag{16}$$

$$\phi = \frac{\beta_\phi s(h+t)}{2L}e_{31} \tag{17}$$

$$C_p = \frac{sL}{2t}\varepsilon_{33}^S \tag{18}$$

Where: β_m, β_k, β_ϕ are Rayleigh Ritz constants; e_{31}, ε_{33}^S are Piezoelectric and clamped dielectric constants ; C_{p11}^E elastic moduli of Piezo ; C_{b11}^E elastic moduli of base plate.

The displacement function of the whole system can be considered in the form of a PDE as

$$M\ddot{u}(t) + \eta\dot{u}(t) + ku(t) + \phi V_p(t) = F(t) \tag{19}$$

The voltage function is considered analogous to the displacement function as

$$-\phi\dot{u}(t) + C_p\dot{V}_p(t) = -I(t) \tag{20}$$

Since we have the condition, $V_c = V_{out}$ by assuming that crippling voltage is negligible as represented in Eq. (22), we have

$$I(t) = C_e\dot{V}_c(t) + \frac{V_c}{R} \tag{21}$$

We have $F(t) = F_0 \sin(\omega t)$ and this is a sine wave operator function for the forced displacement.

Typically, V_c is in DC voltage. Hence

$$V_c(t) = < V_c(t) > + (V_{c,Ripple} = 0) \tag{22}$$

Let the wave function be written in the form of a sinusoidal wave equation with θ being the displacement as $u(t) = u_0 \sin(\omega t - \theta)$ and the voltage function be represented as $V_c(t) = g(\omega t - \theta)$. This converts the final output voltage to the form

$$V_c = \frac{\omega\theta R}{\omega C_p R + \frac{\pi}{2}} \times u_0 \tag{23}$$

Thus, the final output voltage (derived from Eq. (23)) is obtained in mechanical terms of frequency, damping factor and displacement, and electrical factors comprising of equivalent capacitance and load resistance.

3.3 Circuit design

A full wave rectifier, no damping dynamic observer model was made with the error stability function being

$$\lambda_i[A - LC] \leq 0 \tag{24}$$

Here, electrical output is perpendicular to polarisation and applied stress.

Harmonic driving force was modelled as per the dynamic excitation loading as given in Eq. (24).

$$F_i(t) = F_0 \sin(\omega_{dr}t)\,\partial(x - L_{xf})\partial(y - L_{yf}) \tag{25}$$

where, L_{xf} and L_{yf} are representing the displacement values along the length and width, F_0 is amplitude of load function and ω_{dr} is excitation frequency.

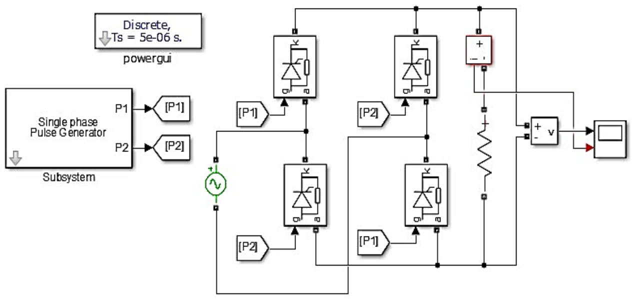

Fig. 4 Implemented circuit design

Table 2 Comparison of frequency values for different material and geometry

Present	Reference	Material
20 Hz	13.1 Hz	Aluminium (Roundy *et al*. 2003)
751.59 Hz	800 Hz	Porcelain (Park *et al*. 2012)

Table 3 Comparison of Power output by varying geometry of the designed analytical model

Present	Literature	% of difference
218.45 μW	242 μW (Roundy *et al*. 2003)	9.731
1.238 μW	1.43 μW (Park *et al*. 2012)	13.426
40300 μW	39000 μW (Kim *et al*. 2005, Li *et al*. 2014)	3.333
49700 μW	52000 μW (Li *et al*. 2014)	4.423
0.89 μW	1 μW (Mitcheson *et al*. 2008 and Williams and Yates 1996)	11
336 μW	400 μW (Himanshu 2013 and Mitcheson *et al*. 2008)	16

4. Model comparison

The designed analytical model is compared to those of the existing model by undertaking the same physical constraints. The results are obtained using a self-made code established in the MATLAB software with the help of proposed higher-order numerical model in conjunction with an FEM model designed using ANSYS Workbench. The convergence and the validation studies of the proposed numerical model has also been checked to show the effectiveness of the presently developed model. In the present analysis, two different types of support conditions are considered for the analysis purpose, which is presented in Tables 2 and 3.

The model has been tested for Aluminium and Porcelain and results are compared. The Aluminium data set is simulated for 1.71 cm × 0.5 cm × 0.3 cm as done in Roundy *et al*. (2003) and the Porcelain data set is simulated for 5.08 cm × 3.18 cm × 0.26 cm as done in (Park *et al*. 2012) for analysis and optimization of energy harvesting micro generator systems.

As observed from the data provided in the tabular form (Tables 2 and 3), it can be concluded that the present analytical model is consistent with the existing experimental values.

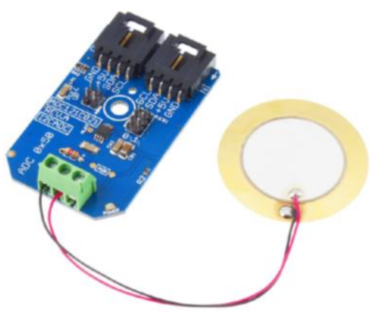

Fig. 5 Transducer circuit of sample piezo layer

5. Prototype model

To show the analytical model validity, a prototype of a harvester has been fabricated. The detail dimension of the fabricated component is listed below for the experimental verification.

1. Base Material Properties:
   a. Young's Modulus: 8 GPa
   b. Density: 1.587 g/cc
   c. Poison's Ratio: 0.17
   d. Dimensions:
      a. L = 150 mm
      b. B = 60 mm
      c. H = 0.8 mm
      d. M = 50 gms
2. PZT Properties:
   a. Young's Modulus: 66 GPa
   b. Dielectric Constant: 1700
   c. Piezoelectric Strain Coefficients:
      1. D31 = 2.2e-11
      2. D33 = -3.0e-11
   d. Dimensions:
      i. L = 50 mm
      ii. B = 10 mm
      iii. H = 0.19 mm
      iv. Piezo Placement from base: 100 mm

Fig. 6 Rectifier circuit of the setup

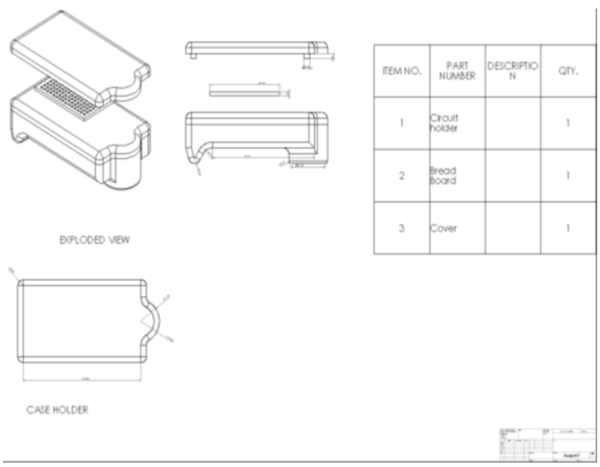

Fig. 7 SolidWorks modelling of prototype frame

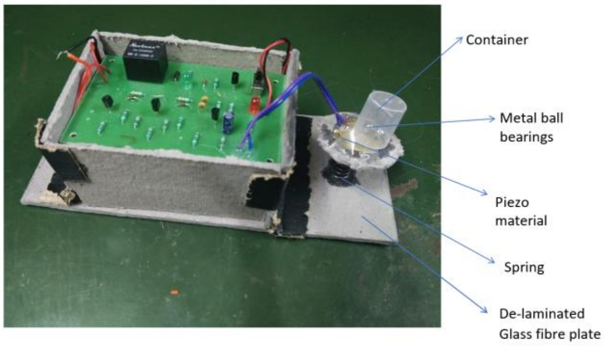

Fig. 8 Actual prototype as per designed constraints

The piezo setup and the corresponding circuit are shown in Figs. 5 and 6, respectively.

The cylindrical dome of the frame contains a rigid spring upon which placed are steel balls of diameter 2 mm each. This type of modelling ensures forced vibration and hence the results are scaled (Josefsson 2014). The actual model is built to a scale of 1:2 with respect to the prototyped format and is shown in Fig. 8.

6. Results and discussions

In the present article, an analytical model is developed to estimate the electrical power via the piezoelectric linkup at low-frequency mode. In this regard, a scaled prototype has been designed using SOLIDWORKS to finalize the dimensions. Further, a harvester has been fabricated and the simulated data verified with the predicted solution. Also, a few relevant parameters affecting the power-output are simulated for the optimal calculation.

6.1 Numerical solution

6.1.1 Frequency v/s Power

The following analysis are carried out under various damping ratios of 0.3, 0.6 and 0.9 respectively. Fig. 9 indicates that the power-output peak is rising at a certain frequency and it corresponds to the 1st modal value.

6.1.2 Resistance v/s Power

To establish the model, a few analysis has been carried out keeping the load resistance as the variable. This is because the resistance of the system mainly blocking the output power. Hence, to obtain the optimal resistance an analytical analysis has been done to improvise the power output data. The initial inclination is due to the direct relationship between the power and the corresponding Load resistance, i.e., as load resistance is increased, power output increases. It reaches a threshold limit of 4387.94ohms. After this threshold limit, voltage starts to drop down as the resistance is further increased. Hence a drop in magnitude of power is seen in Fig. 10.

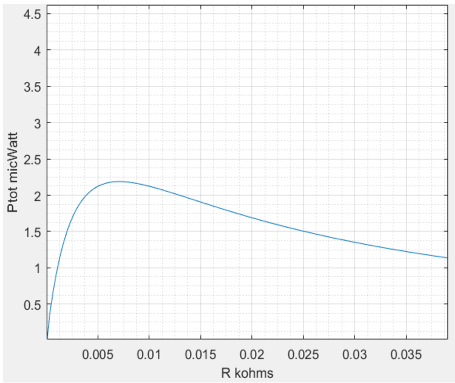

Fig. 10 Resistance v/s Power

6.1.3 Output power v/s Piezo length

Similarly, the power output also depends largely on the piezo placement, i.e., the greater the displacement in the base plate greater is the strain rate response in the piezo layer, hence greater is the voltage generated. Thus, the piezo layer of predefined thickness is to be symmetrically positioned to obtain optimum strain rate response. Fig. 6 indicates the length of the leading edge of the piezo from the fixed base of the cantilever beam. From the graph it is understood that the trailing edge of the piezo must coincide with the trailing edge of the cantilever beam to maximize the power output as depicted in Fig. 11.

6.1.4 Output power v/s Thickness of piezo

From the analysis of the power output formula, it has been observed that, as the thickness of the piezo layer is increased, the strain rate response along ϵ_{31} started to reduce. Due to this, the power output gradually started to reduce after showing a peak value as depicted in Fig. 12.

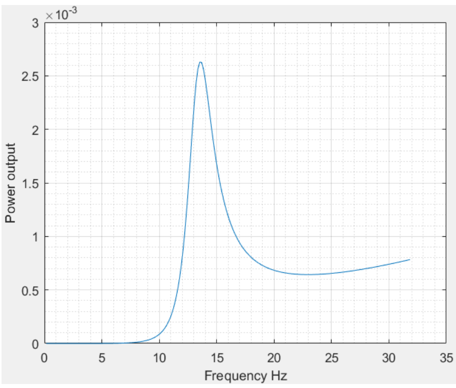

Fig. 9 Freq. v/s Power

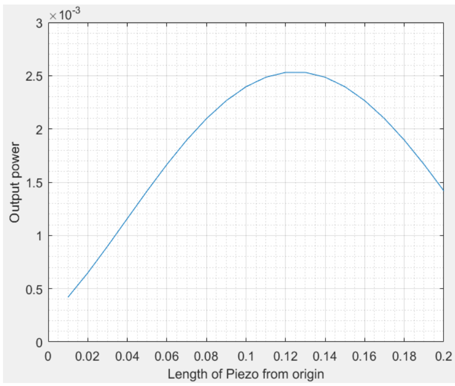

Fig. 11 Piezo length v/s Power

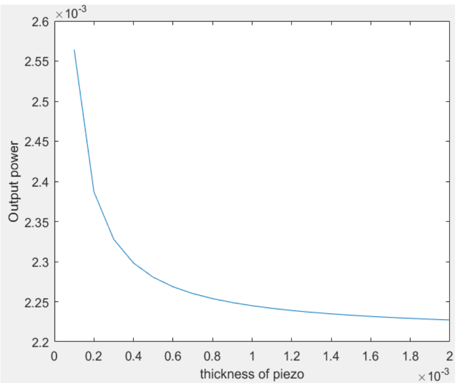

Fig. 12 Piezo thickness v/s Power

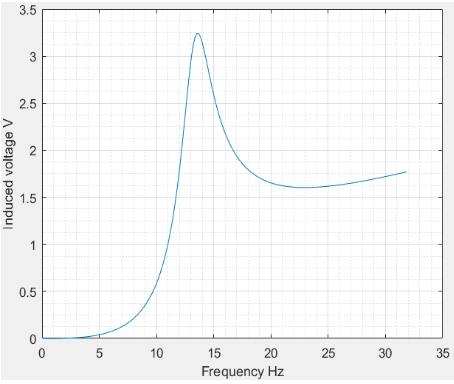

Fig. 13 Induced voltage v/s Frequency

The peak power is obtained when the thickness of the piezo is 0.19 mm and this value of peak power is valued at 2.50 mW.

6.1.5 Frequency v/s Voltage output

The analysis has been carried out to obtain the maximum voltage output using the analytical model. It can be observed that the value is higher at first natural frequency modes. Here, the peak value of voltage is observed to lie at a frequency of 14.16 Hz and its corresponding voltage value of 3.09 Volts as shown in Fig. 13.

6.2 ANSYS simulation

The bimorph actuator model is prepared in ANSYS (workbench 17.1) to evaluate the deflection contours. The base material is chosen as the glass fibre and the dimensioning are given as discussed in Section 4. The deflection contours are obtained for the first two frequency modes. This is because to satisfy the low-frequency band i.e., ≤ 100 Hz.

At the first mode of vibration, the natural frequency observed as 13.45 Hz and the deflection is shown in Fig. 14.

Similarly, the second mode of natural frequency is observed as 84.275 Hz and the deflection pattern shown in Fig. 15.

It can be noticed that the maximum deflection values are always lies at the end of the free side which is highly consistent with the presently derived model considering the

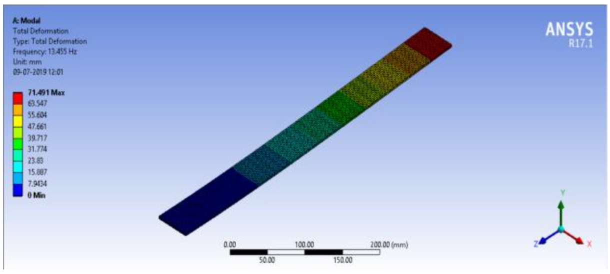

Fig. 14 Deflection contour at 1st mode of vibration

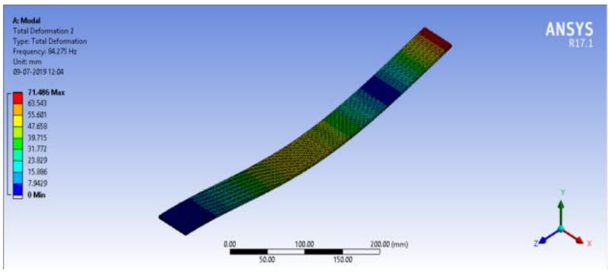

Fig. 15 Deflection contour at 2nd mode of vibration

dimensions as same as the subsection 5.1.3. Thus, employing the external point mass at the free end ensures increased efficiency of the bimorph system by both reducing the coupling factor as well as increasing the frequency output which is justified in Section 5.1.1.

6.3 Experimental validation

The first ten modal values are obtained considering a tip mass (m = 50 grams) and provided in Table. 4. The corresponding experimentation including the test rig can be seen in Fig. 15.

From the table, it can be quite evident that the designed analytical model works for deriving the natural modes of frequency are consistent with a mean margin of error is too small i.e., 2.938%. Also, the simulated frequency response chart obtained from the prototype model utilizing ANSYS is shown in Fig. 16.

6.4 Results comparison

Load resistance = 4000 Ω
Material of the base plate: Glass fibre
Material of the Piezo layer: PZT-5H

Table 4 Comparison of natural frequencies by experimental and theoretical models

Mode	Experimental frequency (Hz)	Theoretical frequency (Hz)	% age error
1.	14.1	13.455	4.79
2.	87.3	84.275	3.58
3.	169.2	166.05	1.29
4.	230.7	236.01	2.25
5.	249.1	255.61	2.55
6.	455.0	462.79	1.68

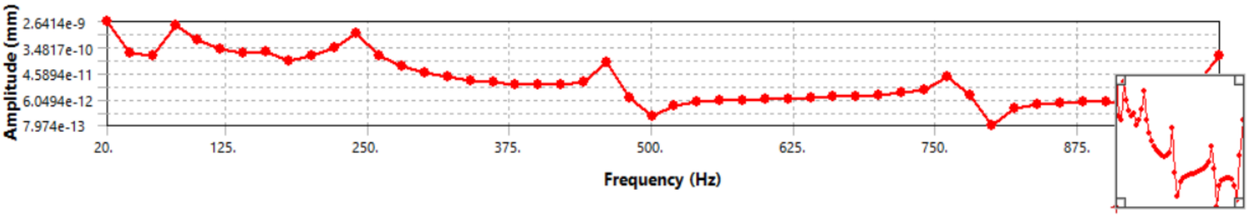

Fig. 16 Amplitude of vibration v/s frequency chart (simulated data)

Table 5 Experimental and theoretical voltage validation with the error percentage

Experimental frequency (Hz)	Analytically obtained frequency (Hz)	Experimentally obtained voltage (V)	Analytically derived voltage (V)	Standard error (% age)
14.1	13.455	2.59	3.09	16.18
87.3	84.275	2.77	2.29	17.22

Table 6 Experimental and theoretical power validation at first and second modes

Mode	Frequency (Hz)	Experimentally obtained power (μW)
1	13.455	2608
2	84.275	2721

Piezo placement: 120 mm from fixed base of cantilever
Final Voltage output: 2.59 Volts (1st mode)
Final Power Output: 2500 Microwatt

The entire prototyping can be constrained in a simple casing which can be attached to the outer portion of vehicle, heavy machinery or any other source of vibration;

The prototype casing consists of a circuit holder that accounts for fixation of the bimorph system, a bread board which accounts for holding all the electrical components and a hard-cardboard cover as depicted in Fig. 7.

Thus, after conducting experimental and theoretical validation of the prototype the marginalised error is found to be 16.71% with respect to the experimented voltage output and the model voltage output.

7. Conclusions

This research reported analytical modelling for energy harvesting through a piezoelectric bimorph beam structure and verified with experimental data. In this regard, a harvesting device has also been fabricated to produce the energy from a low-frequency vibration band with the help of a piezoelectric bimorph actuator. It can be observed that the present model is highly consistent and offers an optimum amount of energy output by utilizing the orthotropic (glass fibre) type base material. Moreover, the experimental results are showing the optimum values of the power for the 2nd mode of vibration instead of 1st mode. The research indicates that the power values can be enhanced further by adopting a high modulator for the amplification of the drawn voltages.

References

Akgöz, B. and Civalek, O. (2013), "Buckling analysis of functionally graded microbeams based on the strain gradient theory", *Acta Mechanica*, **224**(9), 2185-2201. https://doi.org/10.1007/s00707-013-0883-5

Arani, A.G., Kolahchi, R. and Esmailpour, M. (2016), "Nonlinear Vibration Analysis of Piezoelectric Plates Reinforced with Carbon Nanotubes Using DQM", *Smart Struct. Syst., Int. J.*, **18**(4), 787-800. https://doi.org/10.12989/sss.2016.18.4.787

Aridogan, U., Basdogan, I. and Erturk, A. (2014), "Analytical modeling and experimental validation of a structurally integrated piezoelectric energy harvester on a thin plate", *Smart Mater. Struct.*, **23**(4), 045039. https://doi.org/10.1088/0964-1726/23/4/045039

Asghar, S., Naeem, M.N., Hussain, M., Taj, M. and Tounsi, A. (2020), "Prediction and assessment of nonlocal natural frequencies of DWCNTs: Vibration analysis", *Comput. Concrete, Int. J.*, **25**(2), 133-144. https://doi.org/10.12989/cac.2020.25.2.133

Arul, K.T., Ramanjaneyulu, M. and Ramachandra Rao, M.S. (2019), "Energy Harvesting of PZT/PMMA Composite Flexible Films", *Curr. Appl. Phys.*, **19**(4), 375-380. https://doi.org/10.1016/j.cap.2019.01.003

Balamurugan, V. and Narayanan, S. (2009), "Multilayer Higher Order Piezo-Laminated Smart Composite Shell Finite Element and Its Application to Active Vibration Control", *J. Intell. Mater. Syst. Struct.*, **20**(4), 425-441. https://doi.org/10.1177/1045389X08095269

Balubaid, M., Tounsi, A., Dakhel, B. and Mahmoud, S.R. (2019), "Free vibration investigation of FG nanoscale plate using nonlocal two variables integral refined plate theory", *Comput. Concrete, Int. J.*, **24**(6), 579-586. https://doi.org/10.12989/cac.2019.24.6.579

Bedia, W.A., Houari, M.S.A., Bessaim, A., Bousahla, A. ., Tounsi, A., Saeed, T. and Alhodaly, M.S. (2019), "A new hyperbolic two-unknown beam model for bending and buckling analysis of a nonlocal strain gradient nanobeams", *J. Nano Res.*, **57**, 175-191. https://doi.org/10.4028/www.scientific.net/jnanor.57.175

Bellal, M., Hebali, H., Heireche, H., Bousahla, A.A., Tounsi, A., Bourada, F., Mahmoud, S.R., Bedia, E.A. and Tounsi, A. (2020), "Buckling behavior of a single-layered graphene sheet resting on viscoelastic medium via nonlocal four-unknown integral model", *Steel Compos. Struct., Int. J.*, **34**(5), 643-655. https://doi.org/10.12989/scs.2020.34.5.643

Berghouti, H., Adda Bedia, E.A., Benkhedda, A. and Tounsi, A.

(2019), "Vibration analysis of nonlocal porous nanobeams made of functionally graded material", *Adv. Nano Res., Int. J.*, **7**(5), 351-364. https://doi.org/10.12989/anr.2019.7.5.351

Biswal, A.R., Roy, T. and Behera, R.K. (2017), "Optimal Vibration Energy Harvesting from Non-Prismatic Axially Functionally Graded Piezolaminated Cantilever Beam Using Genetic Algorithm", *J. Intell. Mater. Syst. Struct.*, **28**(14), 1957-1976. https://doi.org/10.1177/1045389X16682842

Boukhlif, Z., Bouremana, M., Bourada, F., Bousahla, A.A., Bourada, M., Tounsi, A. and Al-Osta, M.A. (2019), "A simple quasi-3D HSDT for the dynamics analysis of FG thick plate on elastic foundation", *Steel Compos. Struct., Int. J.*, **31**(5), 503-516. https://doi.org/10.12989/scs.2019.31.5.503

Bousahla, A.A., Bourada, F., Mahmoud, S.R., Tounsi, A., Algarni, A., Bedia, E.A.A. and Tounsi, A. (2020), "Buckling and dynamic behavior of the simply supported CNT-RC beams using an integral-first shear deformation theory", *Comput. Concrete, Int. J.*, **25**(2), 155-166. https://doi.org/10.12989/cac.2020.25.2.155

Boutaleb, S., Benrahou, K.H., Bakora, A., Algarni, A., Bousahla, A.A., Tounsi, A. and Mahmoud, S.R. (2019), "Dynamic analysis of nanosize FG rectangular plates based on simple nonlocal quasi 3D HSDT", *Adv. Nano Res., Int. J.*, **7**(3), 191-208. https://doi.org/10.12989/anr.2019.7.3.191

Caliò, R., Rongala, U.B., Camboni, D., Milazzo, M., Stefanini, C., de Petris, G. and Oddo, C.M. (2014), "Piezoelectric Energy Harvesting Solutions", *Sensors*, **14**(3), 4755-4790. https://doi.org/10.3390/s140304755

Civalek, O. and Akgöz, B. (2014), "Longitudinal vibration analysis for microbars based on strain gradient elasticity theory", *J. Vib. Control*, **20**(4), 606-616. https://doi.org/10.1177/1077546312463752

Dagdeviren, C., Yang, B.D., Su, Y., Tran, P.L., Joe, P., Anderson, E., Xia, J., Doraiswamy, V., Dehdashti, B., Feng, X., Lu, B., Poston, R., Khalpey, Z., Ghaffari, R., Huang, Y., Slepian, M.J. and Rogers, J.A. (2014), "Conformal piezoelectric energy harvesting and storage from motions of the heart, lung, and diaphragm", *Proceedings of the National Academy of Sciences*, **111**(5), 1927-1932. https://doi.org/10.1073/pnas.1317233111

Dash, P. and Singh, B.N. (2009), "Nonlinear free vibration of piezoelectric laminated composite plate", *Finite Elem. Anal. Des.*, **45**(10), 686-694. https://doi.org/10.1016/j.finel.2009.05.004

Dechant, E., Fedulov, F., Fetisov, L.Y. and Shamonin, M. (2017), "Bandwidth widening of piezoelectric cantilever beam arrays by mass-tip tuning for low-frequency vibration energy harvesting", *Appl. Sci.*, **7**(12). https://doi.org/10.3390/app7121324

Dutoit, N.E., Brian L.W. and Kim, S.G. (2005), "Design considerations for MEMS-scale piezoelectric mechanical vibration energy harvesters", *Integr. Ferroelectr.*, **71**(1), 121-160. https://doi.org/10.1080/10584580590964574

Erturk, A. and Inman, D.J. (2008), "A Distributed Parameter Electromechanical Model for Cantilevered Piezoelectric Energy Harvesters", *J. Vib. Acoust.*, **130**(4), 041002. https://doi.org/10.1115/1.2890402

Erturk, A. and Inman, D.J. (2009), "An experimentally validated bimorph cantilever model for piezoelectric energy harvesting from base excitations", *Smart Mater. Struct.*, **18**(2). https://doi.org/10.1088/0964-1726/18/2/025009

Glynne-Jones, P., Tudor, M.J., Beeby, S.P. and White, N.M. (2004), "An electromagnetic, vibration-powered generator for intelligent sensor systems", *Sensors Actuators A Phys.*, **110**(1-3), 344-349. https://doi.org/10.1016/j.sna.2003.09.045

Himanshu, P. (2013), "Piezoelectric Transduction Mechanism for Vibration Based Energy Harvesting", NITR M.Tech Thesis; NIT Rourkela, pp. 1-72.

Hung, E.S. and Senturia, S.D. (1999), "Extending the travel range of analog-tuned electrostatic actuators", *J. Microelectromech. Syst*, **8**(4), 497-505. https://doi.org/10.1109/84.809065

Hussain, M., Naeem, M.N., Tounsi, A. and Taj, M. (2019), "Nonlocal effect on the vibration of armchair and zigzag SWCNTs with bending rigidity", *Adv. Nano Res., Int. J.*, **7**(6), 431-442. https://doi.org/10.12989/anr.2019.7.6.431

Josefsson, A. (2014), *An Early Product Development Project at a Start-up Company*.

Kaddari, M., Kaci, A., Bousahla, A.A., Tounsi, A., Bourada, F., Tounsi, A., Bedia, E.A.A. and Al-Osta, M.A. (2020), "A study on the structural behaviour of functionally graded porous plates on elastic foundation using a new quasi-3D model: Bending and free vibration analysis", *Comput. Concrete, Int. J.*, **25**(1), 37-57. https://doi.org/10.12989/cac.2020.25.1.037

Karami, B., Janghorban, M. and Tounsi, A. (2019a), "Galerkin's approach for buckling analysis of functionally graded anisotropic nanoplates/different boundary conditions", *Eng. Compos.*, **35**, 1297-1316. https://doi.org/10.1007/s00366-018-0664-9

Karami, B., Janghorban, M. and Tounsi, A. (2019b), "Wave propagation of functionally graded anisotropic nanoplates resting on Winkler-Pasternak foundation", *Struct. Eng. Mech., Int. J.*, **70**(1), 55-66. https://doi.org/10.12989/sem.2019.70.1.055

Karami, B., Shahsavari, D., Janghorban, M. and Tounsi, A. (2019c), "Resonance behavior of functionally graded polymer composite nanoplates reinforced with graphene nanoplatelets", *Int. J. Mech. Sci.*, **156**, 94-105. https://doi.org/10.1016/j.ijmecsci.2019.03.036

Karami, B., Janghorban, M. and Tounsi, A. (2019d), "On exact wave propagation analysis of triclinic material using three-dimensional bi-Helmholtz gradient plate model", *Struct. Eng. Mech., Int. J.*, **69**(5), 487-497. https://doi.org/10.12989/sem.2019.69.5.487

Karami, B., Janghorban, M. and Tounsi, A. (2019e), "On pre-stressed functionally graded anisotropic nanoshell in magnetic field", *J Braz. Soc. Mech. Sci. Eng.*, **41**, 495. https://doi.org/10.1007/s40430-019-1996-0

Khalatkar, A., Gupta, V.K. and Agrawal, A. (2014), "Analytical, FEA, and experimental comparisons of piezoelectric energy harvesting using engine vibrations", *Smart Mater. Res.*, 1-8. https://doi.org/10.1155/2014/741280

Kim, H.W., Priya, S., Uchino, K. and Newnham, R.E. (2005), "Piezoelectric Energy Harvesting under High Pre-Stressed Cyclic Vibrations", *J. Electroceram.*, **15**(1), 27-34. https://doi.org/10.1007/s10832-005-0897-z

Kim, J.E., Kim, H., Yoon, H., Kim, Y.Y. and Youn, B.D. (2015), "An Energy conversion model for cantilevered piezoelectric vibration energy harvesters using only measurable parameters", *Int. J. of Precis. Eng. Manuf.-Green Tech.*, **2**, 51-57. https://doi.org/10.1007/s40684-015-0007-x

Kong, L.B., Li, T., Hng, H.H., Boey, F., Zhang, T. and Li, S. (2014), *Waste Energy Harvesting*, (Vol. 24), Springer-Verlag Berlin Heidelberg, Berlin, Heidelberg, Germany.

Kundu, S. and Nemade, H.B. (2016), "Modeling and simulation of a piezoelectric vibration energy harvester", *Procedia Eng.*, **144**, 568-575. https://doi.org/10.1016/j.proeng.2016.05.043

Li, X., Bhushan, B., Takashima, K., Baek, C.-W. and Kim, Y.-K. (2003), "Mechanical characterization of micro/nanoscale structures for MEMS/NEMS applications using nanoindentation techniques", *Ultramicroscopy*, **97**(1-4), 481-494. https://doi.org/10.1016/S0304-3991(03)00077-9

Li, H., Tian, C. and Deng, Z.D. (2014), "Energy harvesting from low frequency applications using piezoelectric materials", *Appl. Phys. Rev.*, **1**(4), 041301. https://doi.org/10.1063/1.4900845

Mitcheson, P.D., Miao, P., Stark, B.H., Yeatman, E.M., Holmes, A.S. and Green, T.C. (2004), "MEMS Electrostatic Micropower Generator for Low Frequency Operation", *Sensors Actuat. A Phys.*, **115**(2-3), 523-529. https://doi.org/10.1016/j.sna.2004.04.026

Mitcheson, P.D., Yeatman, E.M., Rao, G.K., Holmes, A.S. and

Green, T.C. (2008), “Energy harvesting from human and machine motion for wireless electronic devices”, *Proc. IEEE*, **96**(9), 1457-1486. https://doi.org/10.1109/JPROC.2008.927494

Mahmoudi, A., Benyoucef, S., Tounsi, A., Benachour, A., Bedia, E.A.A. and Mahmoud, S.R. (2017), “A refined quasi-3D shear deformation theory for thermo-mechanical behavior of functionally graded sandwich plates on elastic foundations”, *J. Sandw. Struct. Mater.*, **21**(6), 1906-1926. https://doi.org/10.1177/1099636217727577

Mohammadzadeh-Keleshteri, M., Asadi, H. and Aghdam, M.M. (2017), “Geometrical Nonlinear Free Vibration Responses of FG-CNT Reinforced Composite Annular Sector Plates Integrated with Piezoelectric Layers”, *Compos. Struct.*, **171**, 100-112. https://doi.org/10.1016/j.compstruct.2017.01.048

Moser, Y. and Gijs, M.A.M. (2007), “Miniaturized Flexible Temperature Sensor”, *J. Microelectromech. Syst.*, **16**(6), 1349-1354. https://doi.org/10.1109/JMEMS.2007.908437

Motezaker, M. and Eyvazian, E. (2020), “Post-buckling analysis of Mindlin Cut out-plate reinforced by FG-CNTs”, *Steel Compos. Struct.*, *Int. J.*, **34**(2), 289-297. https://doi.org/10.12989/scs.2020.34.2.289

Motezaker, M., Jamali, M. and Kolahchi, R. (2020), “Application of differential cubature method for nonlocal vibration, buckling and bending response of annular nanoplates integrated by piezoelectric layers based on surface-higher order nonlocal-piezoelasticity theory”, *J Computat. Appl. Mathe.*, **369**, 112625. https://doi.org/10.1016/j.cam.2019.112625

Muralt, P., Marzencki, M., Belgacem, B., Calame, F. and Basrour, S. (2009), “Vibration energy harvesting with PZT micro device”, *Procedia Chem.*, **1**(1), 1191-1194. https://doi.org/10.1016/j.proche.2009.07.297

Najini, H. and Muthukumaraswamy, S.A. (2017), “Piezoelectric energy generation from vehicle traffic with technoeconomic analysis”, *J. Renew. Energy*, 1-16. https://doi.org/10.1155/2017/9643858

Othman, A. (2017), “Modeling of piezoelectric energy harvesting system embedded in soldier’s boot using Matlab/Simulink”, *Proceedings of 2017 International Conference on Military Technologies* (*ICMT*), pp. 787-792. https://doi.org/10.1109/MILTECHS.2017.7988862

Panda, P.K., Sahoo, B., Ramakrishna, J., Manoj, B. and Prasada Rao, D.S.D. (2018), “Recent Studies on Vibrational Energy Harvesting of PZT Materials”, *Mater. Today Proc.*, **5**(10), 21512-21516. https://doi.org/10.1016/j.matpr.2018.06.562

Park, J., Lee, S. and Kwak, B.M. (2012), “Design optimization of piezoelectric energy harvester subject to tip excitation”, *J. Mech. Sci. Technol.*, **26**(1), 137-143. https://doi.org/10.1007/s12206-011-0910-1

Rafiee, M., Mohammadi, M., Aragh, B.S. and Yaghoobi, H. (2013), “Nonlinear free and forced thermo-electro-aero-elastic vibration and dynamic response of piezoelectric functionally graded laminated composite shells, Part II: Numerical results”, *Compos. Struct.*, **103**, 188-196. https://doi.org/10.1016/j.compstruct.2012.12.050

Rahmani, M.C., Kaci, A., Bousahla, A.A., Bourada, F., Tounsi, A., Bedia, E.A.A., Mahmoud, S.R., Benrahou, K.H. and Tounsi, A. (2020), “Influence of boundary conditions on the bending and free vibration behavior of FGM sandwich plates using a four-unknown refined integral plate theory”, *Comput. Concrete*, *Int. J.*, **25**(3), 225-244. https://doi.org/10.12989/cac.2020.25.3.225

Roundy, S. and Wright, P.K. (2004), “A piezoelectric vibration based generator for wireless electronics”, *Smart Mater. Struct.*, **13**(5), 1131-1142. https://doi.org/10.1088/0964-1726/13/5/018

Roundy, S., Wright, P.K. and Rabaey, J. (2003), “A study of low level vibrations as a power source for wireless sensor nodes”, *Comput. Commun.*, **26**(11), 1131-1144. https://doi.org/10.1016/S0140-3664(02)00248-7

Sahla, Meriem., Saidi, H., Draiche, K., Bousahla, A.A., Bourada, F. and Tounsi, A. (2019), “Free vibration analysis of angle-ply laminated composite and soft core sandwich plates”, *Steel Compos. Struct.*, *Int. J.*, **33**(5), 663-679. https://doi.org/10.12989/scs.2019.33.5.663

Semmah, A., Heireche, H., Bousahla, A.A. and Tounsi, A. (2019), “Thermal buckling analysis of SWBNNT on Winkler foundation by non local FSDT”, *Adv. Nano Res.*, *Int. J.*, **7**(2), 89-98. https://doi.org/10.12989/anr.2019.7.2.089

Shen, D., Park, J.-H., Noh, J.H., Choe, S.-Y., Kim, S.-H., Wikle, H.C. and Kim, D.-J. (2009), “Micromachined PZT cantilever based on SOI structure for low frequency vibration energy harvesting”, *Sensors Actuators A Phys.*, **154**(1), 103-108. https://doi.org/10.1016/j.sna.2009.06.007

Shu, Y.C. and Lien, I.C. (2006), “Analysis of power output for piezoelectric energy harvesting systems”, *Smart Mater. Struct.*, **15**(6), 1499. https://doi.org/10.1088/0964-1726/15/6/001

Shutao, P., Zheng X., Jing, S., Yong, Z., Liang, Z., Jihe, Z., Deng S., Mingfang, C., Wei, X. and Ke, P. (2012), “Modeling of a micro-cantilevered piezo-actuator considering the buffer layer and electrodes”, *J. Micromech. Microeng.*, **22**(6). https://doi.org/10.1088/0960-1317/22/6/065005

Singh, V.K. and Panda, S.K. (2017), “Geometrical nonlinear free vibration analysis of laminated composite doubly curved shell panels embedded with piezoelectric layers”, *J. Vib. Control*, **23**(13), 2078-2093. https://doi.org/10.1177/1077546315609988

Singh, V.K., Mahapatra, T.R. and Panda, S.K. (2016), “Nonlinear Transient Analysis of Smart Laminated Composite Plate Integrated with PVDF Sensor and AFC Actuator”, *Compos. Struct.*, **157**, 121-130. https://doi.org/10.1016/j.compstruct.2016.08.020

Taj, M., Majeed, A., Hussain, M., Naeem, M.N., Safeer, M., Ahmad, M. and Tounsi, A. (2020), “Non-local orthotropic elastic shell model for vibration analysis of protein microtubules”, *Comput. Concrete*, *Int. J.*, **25**(3), 245-253. https://doi.org/10.12989/cac.2020.25.3.245

Tlidji, Y., Zidour, M., Draiche, K., Safa, A., Bourada, M., Tounsi, A., Bousahla, A.A. and Mahmoud, S.R. (2019), “Vibration analysis of different material distributions of functionally graded microbeam”, *Struct. Eng. Mech*, *Int. J.*, **69**(6), 637-649. https://doi.org/10.12989/sem.2019.69.6.637

Williams, C.B. and Yates, R.B. (1996), “Analysis of a micro-electric generator for microsystems”, *Sensors Actuators A Phys.*, **52**(1-3), 8-11. https://doi.org/10.1016/0924-4247(96)80118-X

Yang, B. (2010), “Hybrid energy harvester based on piezoelectric and electromagnetic mechanisms”, *J. Micro/Nanolithogr. MEMS, MOEMS*, **9**(2), 023002. https://doi.org/10.1117/1.3373516

Zaoui, F.Z., Ouinas, D. and Tounsi, A. (2019), “New 2D and quasi-3D shear deformation theories for free vibration of functionally graded plates on elastic foundations”, *Compos. Part B: Eng.*, **159**, 231-247. https://doi.org/10.1016/j.compositesb.2018.09.051

Zeng, S., Zhang, C., Wang, K., Wang, B. and Sun, L. (2018), “Analysis of delamination of unimorph cantilever piezoelectric energy harvesters”, *J. Intell. Mater. Syst. Struct.*, **29**(9), 1875-1883. https://doi.org/10.1177/1045389X17754273

Zhu, M., Worthington, E. and Njuguna, J. (2009), “Analyses of power output of piezoelectric energy-harvesting devices directly connected to a load resistor using a coupled piezoelectric-circuit finite element method”, *IEEE Trans. Ultrason. Ferroelectr. Freq. Control*, **56**(7), 1309-1317. https://doi.org/10.1109/TUFFC.2009.1187

CC